Cell, Vol. 110, 649–660, September 6, 2002, Copyright ©2002 by Cell Press

Sidekicks: Synaptic Adhesion Molecules that Promote Lamina-Specific Connectivity in the Retina

Masahito Yamagata, Joshua A. Weiner, and Joshua R. Sanes[1]
Department of Anatomy and Neurobiology
School of Medicine
Washington University
Saint Louis, Missouri 63110

Summary

A major determinant of specific connectivity in the central nervous system is that synapses made by distinct afferent populations are restricted to particular laminae in their target area. We identify Sidekick (Sdk)-1 and -2, homologous transmembrane immunoglobulin superfamily molecules that mediate homophilic adhesion in vitro and direct laminar targeting of neurites in vivo. *sdk-1* and *-2* are expressed by nonoverlapping subsets of retinal neurons; each *sdk* is expressed by presynaptic (amacrine and bipolar) and postsynaptic (ganglion) cells that project to common inner plexiform (synaptic) sublaminae. Sdk proteins are concentrated at synaptic sites, and Sdk-positive synapses are restricted to the 2 (of ≥10) sublaminae to which *sdk*-expressing cells project. Ectopic expression of Sdk in Sdk-negative cells redirects their processes to a Sdk-positive sublamina. These results implicate Sdks as determinants of lamina-specific synaptic connectivity.

Introduction

Specific connectivity, the hallmark of the nervous system, arises as the culmination of numerous processes, including generation of appropriate neuronal types, migration of neurons to nuclei or laminae, growth of axons to target areas, and formation of synapses on particular neurons within the targets (reviewed in Holt and Harris, 1998; Benson et al., 2001). Of these steps, the last is currently the least well understood.

Here, we focus on a form of synaptic specificity that involves the laminar restriction of an axon's terminals. Many regions of the vertebrate brain are divided into multiple laminae, each of which bears a unique assortment of neuronal types. Axons entering laminated areas often confine their synaptic connections to just one lamina; distinct afferent populations terminate in different laminae, where they synapse on interneurons confined to those laminae or on lamina-restricted segments of dendrites that themselves span multiple laminae. Such laminar restrictions are simple to observe and so common that they appear to be major determinants of synaptic specificity (reviewed in Sanes and Yamagata, 1999).

Retinal ganglion cells (RGCs) are useful for analysis of laminar specificity because both their axons and dendrites make striking laminar choices. RGCs are the sole output neurons of the retina and, in most vertebrates, project mainly to the optic tectum. Terminals of retinal axons are confined to just a few of the tectal laminae—3 of 16 in chick—and some tectal cues have been identified that promote axonal arborization in these retinorecipient laminae (Yamagata and Sanes, 1995a; Inoue and Sanes, 1997). Moreover, each individual axon synapses in just a single retinorecipient lamina, and RGCs that project to specific laminae have distinct neurochemical identities (Karten et al., 1982; Yamagata and Sanes, 1995b).

Within the retina, RGC somata are confined to the innermost layer (the ganglion cell layer, GCL), and their dendrites arborize in the adjacent inner plexiform layer (IPL), where they receive inputs from amacrine and bipolar neurons residing in the overlying inner nuclear layer (Masland, 2001). Like their axons, RGC dendrites are further stratified: dendrites of distinct classes ramify in narrow sublaminae within the IPL (Cajal, 1893; Karten et al., 1982). Recent physiological analyses indicate that amacrines and bipolars bring uniquely computed representations of the visual world to at least ten parallel sublaminae; each representation is conveyed to the brain through the subset of RGCs whose dendrites ramify in that sublamina (Roska and Werblin, 2001). Thus, lamina-specific patterns of synaptic connectivity are critical for information processing.

We hypothesized that genes responsible for lamina-specific synaptic choices of RGC axons and dendrites would be selectively expressed by subsets of RGCs during the period when laminae are forming. In a screen for such genes, we identified two vertebrate orthologs of *Drosophila sidekick* (*sdk*) which was, remarkably, identified in a screen for determinants of retinal patterning (Nguyen et al., 1997). We show here that Sdk-1 and Sdk-2 are homophilic adhesion molecules expressed by nonoverlapping subsets of retinal neurons. Sdk proteins are concentrated at synapses that connect Sdk-expressing pre- and postsynaptic partners, suggesting that their homophilic adhesion properties promote formation or stabilization of synapses. In the IPL, Sdk-positive synapses are confined to specific sublaminae, and ectopic expression of Sdk in Sdk-negative cells diverts their arbors to Sdk-positive sublaminae. Together, these results suggest that Sdks are target recognition molecules that mediate lamina-specific synaptogenesis.

Results

Identification of Vertebrate *sidekicks*

To identify genes selectively expressed by RGC subsets, we isolated single RGCs that differed in size and cell-surface properties, amplified cDNA from them by RT-PCR, and constructed libraries from the cDNA (Dulac and Axel, 1995; see Experimental Procedures). Clones from one library were then screened with probes from two RT-PCR products, one that had been used to construct the library being screened and one from an RGC of a distinct type. cDNAs from clones that hybridized

[1]Correspondence: sanesj@pcg.wustl.edu

better to "their own" probe than to the other probe were tested by in situ hybridization to retinal sections, and those that hybridized to subsets of RGCs were analyzed further. One such 417 bp fragment was used to screen a chicken retinal cDNA library, leading eventually to isolation of clones spanning a 6507 nt (2169 aa) open reading frame (Figure 1A). This novel sequence was homologous to that of the *Drosophila melanogaster sidekick* (*sdk*) gene (Nguyen et al., 1997; discussed below). We therefore call the gene chicken *sdk-1*.

Searches of databases revealed one *sdk*-like sequence in *C. elegans* and two each in mice and humans. Of the mammalian *sdk* genes, one was clearly more related to chick *sdk-1* than the other. Using the more divergent mouse *sdk* cDNA as a probe, we cloned a second chick gene, also expressed by a subset of RGCs, which we call *sdk-2* (Figure 1A). Sdk-1 and -2 are 59% identical to each other at the amino acid level, and both are ~35% identical to *Drosophila* Sdk (Figure 1B). One homolog in each vertebrate species corresponds to *sdk-1* and the other to *sdk-2* (Figure 1C). No additional close relatives were found in any species. The Celera database (http://www.celera.com) indicates that the *sdk-1* gene is on human chromosome 7p22 and mouse chromosome 5, and *sdk-2* is on human chromosome 17q24-25 and mouse chromosome 11.

Predicted protein products of the vertebrate, *Drosophila*, and *C. elegans sdk* genes are similar in size and identical in domain organization (Figure 1B). From amino to carboxyl terminus, each consists of: (1) a signal sequence, (2) 6 immunoglobulin (Ig) C2 motifs, (3) 13 fibronectin type III (FN-III) repeats, (4) a single transmembrane domain, and (5) a ~200 aa cytoplasmic domain (Figure 1B). Interestingly, the C-terminal hexapeptide, GFSSFV, is conserved in all Sdks of all the species known (Figure 1D). This sequence contains the canonical carboxy-terminal motif (S/TxV) for binding to PDZ domain-containing scaffold proteins, several of which are concentrated at synaptic sites (Sheng and Sala, 2001). This unusual degree of conservation across three phyla raises the possibility that mechanisms of sdk localization and signaling are also evolutionarily conserved.

Complementary Expression of *sdk-1* and *-2*

To ask whether *sdks* are expressed in distinct subsets of retinal cells, we optimized a double-label fluorescent in situ hybridization protocol for application to genes expressed at low levels. Neither *sdk* gene was detectably expressed during the early stages of retinal neurogenesis and neuronal migration, implying that they are not required for these processes. By embryonic day (E) 10, however, both *sdk-1* and *sdk-2* transcripts were present in the central retina, which develops first. Activation of *sdk* expression occurs just as the GCL is being separated from the inner nuclear layer (which contains horizontal, bipolar, and amacrine cells) by the nascent IPL (which contains synapses of bipolar and amacrine cells with RGCs). By E13, *sdk-1* and *sdk-2* were readily detectable throughout the retina, and their qualitative patterns of expression did not change at least until post-hatching day (P) 2 (hatching is at E21), nor did they differ greatly between central and peripheral retina or along the dorsoventral or nasotemporal axes (Figure 2 and data not shown).

At each stage, *sdk-1* and *sdk-2* were expressed in nonoverlapping subsets of cells. In the outer nuclear layer, which contains photoreceptors, and in the middle portion of the inner nuclear layer, which is rich in bipolar and Muller glia somata, *sdk-2*-positive cells predominated. In the GCL, however, and in the remainder of the inner nuclear layer, *sdk-1*- and *sdk-2*-positive cells were intermingled. In the GCL, each *sdk* was expressed in ~25% of cells, as judged by triple-labeling with a nuclear dye. If the two genes were expressed in random subsets, ~6% of cells would have been both *sdk-1* and *sdk-2* positive, but the number of double-labeled cells was <1% and the few detected were probably artifacts due to superposition of cells. Likewise, no cells were convincingly double-labeled in the inner nuclear layer.

Most cells in the chick GCL are RGCs, but ~15% are displaced amacrine cells (Millar et al., 1987). To test the possibility that *sdk*-expressing cells in the GCL were amacrines, we performed double-label analysis in which each *sdk* probe was combined with a probe for the RGC-specific marker thy-1 (Sheppard et al., 1991). Most of the *sdk*-positive cells in the ganglion cell layer were RGCs (not shown).

Sdks Are Concentrated at Synapses

To localize Sdk proteins, we generated monoclonal antibodies against recombinant fragments of the Sdk-1 and -2 extracellular domains. One antibody specific for each sdk was used for immunohistochemical studies (Figure 3A). Both Sdk proteins migrated at sizes consistent with molecular weights predicted from the cDNA sequences (239,479 for sdk-1 and 243,100 for sdk-2).

Using these antibodies, we found that Sdk proteins were highly concentrated in the synapse-rich plexiform layers with no immunoreactivity detected on somata or proximal processes (Figure 3B). In the IPL, both Sdks were further restricted to two sublaminae, which are described below. Sdks were detectable by E11 (Sdk-2) or E13 (Sdk-1) and thus were present during the period that sublamination was occurring. Consistent with results from in situ hybridization (Figure 2), levels of Sdk-1 decreased as development proceeded; levels of Sdk-2 decreased in the IPL but increased in the outer plexiform layer during this period. Immunoreactivity remained confined to synapse-rich regions throughout development.

To ask whether Sdk proteins are localized at synaptic sites, we focused on the outer plexiform layer because the synapses it contains are large. Sections were triple-labeled with anti-Sdk-2; anti-synaptophysin, a component of synaptic vesicles concentrated in nerve terminals; and phalloidin, a specific ligand for actin, which is concentrated in the postsynaptic apparatus. Confocal analysis revealed that the Sdk-2 extracellular domain resides between the pre- and postsynaptic specializations (Figure 3C), presumably in the synaptic cleft. Synapses in the IPL were too small to permit similar analysis, and our antibodies proved unsuitable for electron microscopic immunohistochemistry. However, results in this region were consistent with those obtained in the outer plexiform layer: anti-Sdk-1 and anti-Sdk-2 labeled small

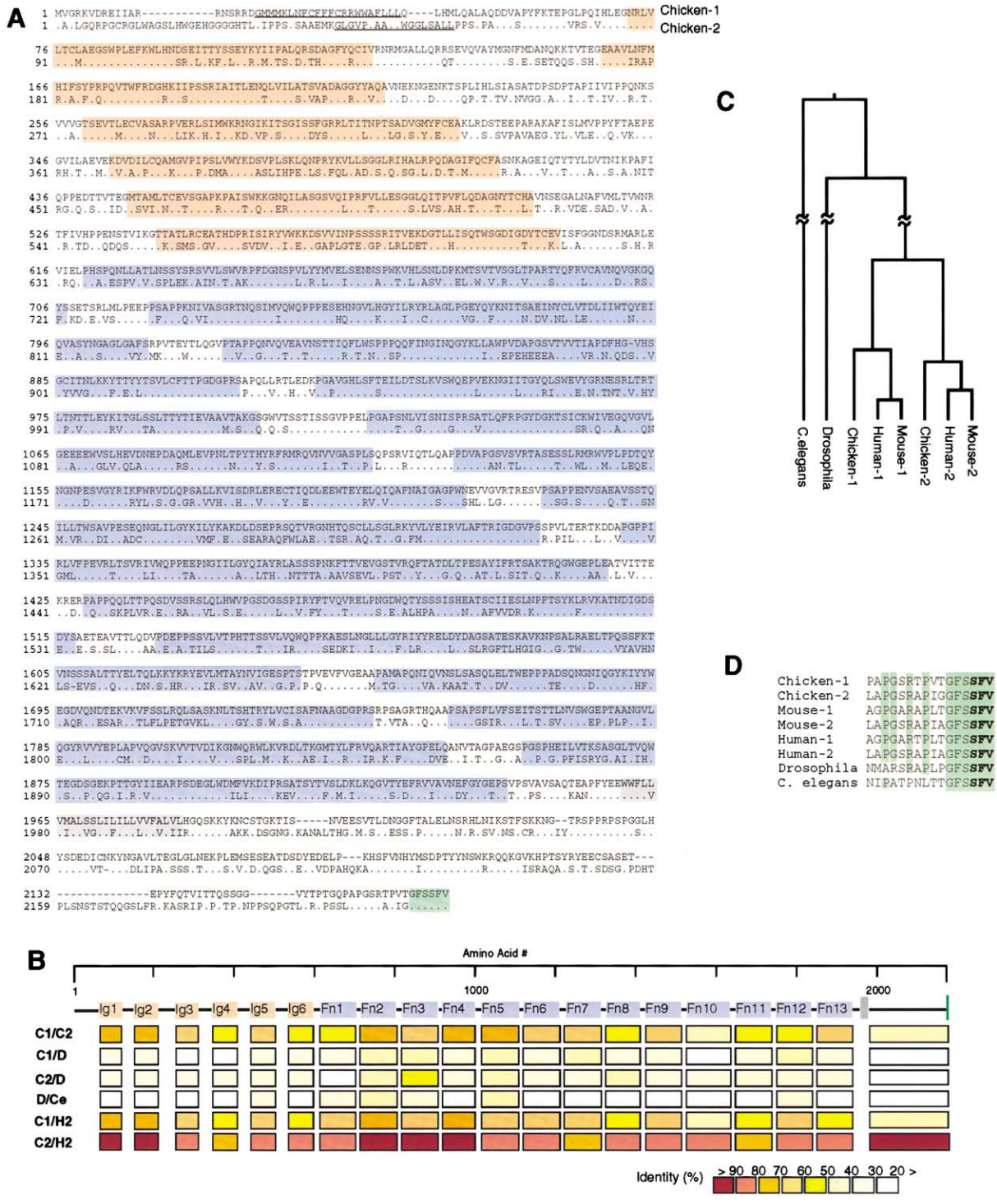

Figure 1. Sequence and Structure of Sdks

(A) Amino acid sequences of chicken Sdk-1 and Sdk-2, deduced from cDNA sequence. Identical residues are shown by dots. The predicted signal peptide is underlined, Ig C2 motifs are orange, FN-III repeats are blue, the transmembrane domain is gray, and the conserved C-terminal sequence is green.

(B) Domain structure and local homology of Sdks. Domains of selected pairs are compared, using a color scale to indicate percent amino acid identity. D, *Drosophila* Sdk; C1, chicken Sdk-1; C2, chicken Sdk-2; H2, human Sdk-2; Ce, *C. elegans* Sdk.

(C) Phylogenic dendrogram of Sdk proteins. This dendrogram is based on the fifth FN-III repeat, which is well conserved among all Sdks. Similar results were obtained using other domains.

(D) C termini of Sdks from three phyla, with identical residues shaded. The last three amino acids correspond to the canonical motif (S/TxV) for binding PDZ scaffold proteins, and preceding residues are known to influence the specificity of PDZ domain interactions.

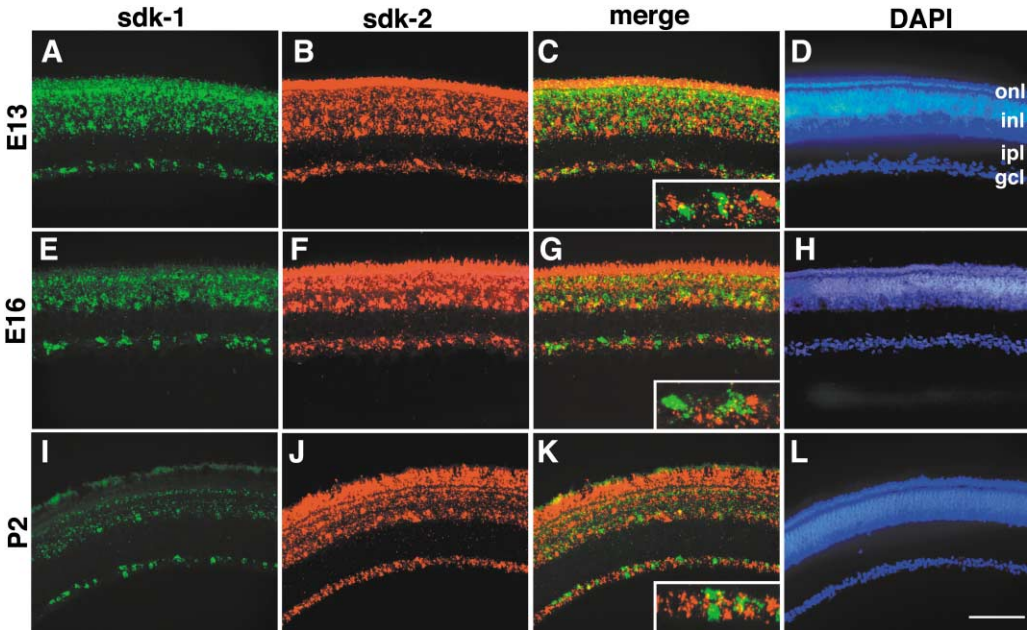

Figure 2. Distinct Retinal Cells Express *sdk-1* and *sdk-2*

Sections of chick retina from the ages indicated were subjected to fluorescent in situ hybridization with probes to *sdk-1* (green) and *sdk-2* (red); nuclei were counterstained with DAPI (blue). Insets show ganglion cell layer (gcl) at higher power, to demonstrate that *sdk-1*- and *sdk-2*-positive subsets are nonoverlapping. Nonoverlapping subsets are also visible in the inner nuclear layer (inl), whereas *sdk-2* expression predominates in the outer nuclear layer (onl). Ipl, inner plexiform layer. Bar equals 100 μm.

puncta coincident with or directly apposed to synaptophysin- and actin-positive varicosities (Figure 3D and data not shown).

Sdks Mediate Homophilic Adhesion

If Sdks are present in synaptic membranes, they might contribute to synaptic adhesion. To determine whether Sdks are adhesive, we produced soluble extracellular domains of Sdk proteins in cultured cells, coated fluorescent beads with purified protein, and assessed aggregation of the particles.

When gently rotated at room temperature, Sdk-1- and Sdk-2-coated beads aggregated within 1 hr (Figures 4A and 4B). Aggregation was Sdk dependent because beads coated with albumin or with purified, recombinant alkaline phosphatase (AP; produced and purified in parallel with the Sdk) remained dispersed (Figure 4C and data not shown). To guard against the possibility that Sdk-coated beads nonspecifically recruited particles into aggregates, we mixed Sdk-1-coated green beads with AP-coated red beads. In this case, Sdk-1 beads aggregated while AP-coated beads remained dispersed (Figure 4D). As expected for Ig superfamily molecules, Sdk-coated beads aggregated well in divalent cations-free medium (data not shown). These results demonstrate that Sdks interact homophilically, and thus could mediate adhesion between opposed Sdk-positive pre- and postsynaptic elements.

To ask whether Sdk-1 and Sdk-2 can adhere to each other, we mixed Sdk-1-coated red beads with Sdk-2-coated green beads. The two types of beads formed separate aggregates (Figure 4E). Likewise, green Sdk-1 and red Sdk-2 remained segregated. The two types of beads are compatible, because mixed (yellow) aggregates formed readily when red and green beads were coated with Sdk-2 (Figure 4F). Thus, heterophilic interactions between Sdks, if they occurred at all, were much weaker than homophilic interactions.

Sdks Mark Specific Plexiform Sublaminae

To test the possibility that homophilic (or other) interactions of Sdks affect the laminar restriction of neurites in the IPL, we first mapped the sublaminae in which they were concentrated. We used a classification system that divides the IPL into five sublaminae, S1–S5. Sdk-2 was most highly concentrated in S2 (36% ± 5% of the distance from the margin of the inner nuclear layer to that of the GCL, mean ± SD), with lower levels in S4 (66% ± 2%), whereas the opposite was true for Sdk-1 (Figure 3B). Neither Sdk was detectable in S1, S3, or S5. It was apparent, however, that Sdk-positive bands occupied only a small fraction of S2 and S4. This highly restricted pattern raised the possibility that Sdks were associated with very specific subsets of synapses. We therefore characterized Sdk-positive bands (Figures 5A and 5B). These studies were performed at E15, after sublamination had occurred and when Sdk levels were at their peak.

VVA-B4, a lectin that recognizes β-N-acetyl-galactosaminyl-terminated oligosaccharides (Scott et al., 1988), stained narrow bands in S2, S3, and S4; the VVA-B4-positive bands in S2 and S4 were coincident with the Sdk-positive bands. Double staining with anti-Sdk-1 and anti-Sdk-2 was not possible because both antibodies were of the same subclass, but staining with each antibody plus VVA-B4 demonstrated that Sdk-1 and Sdk-2

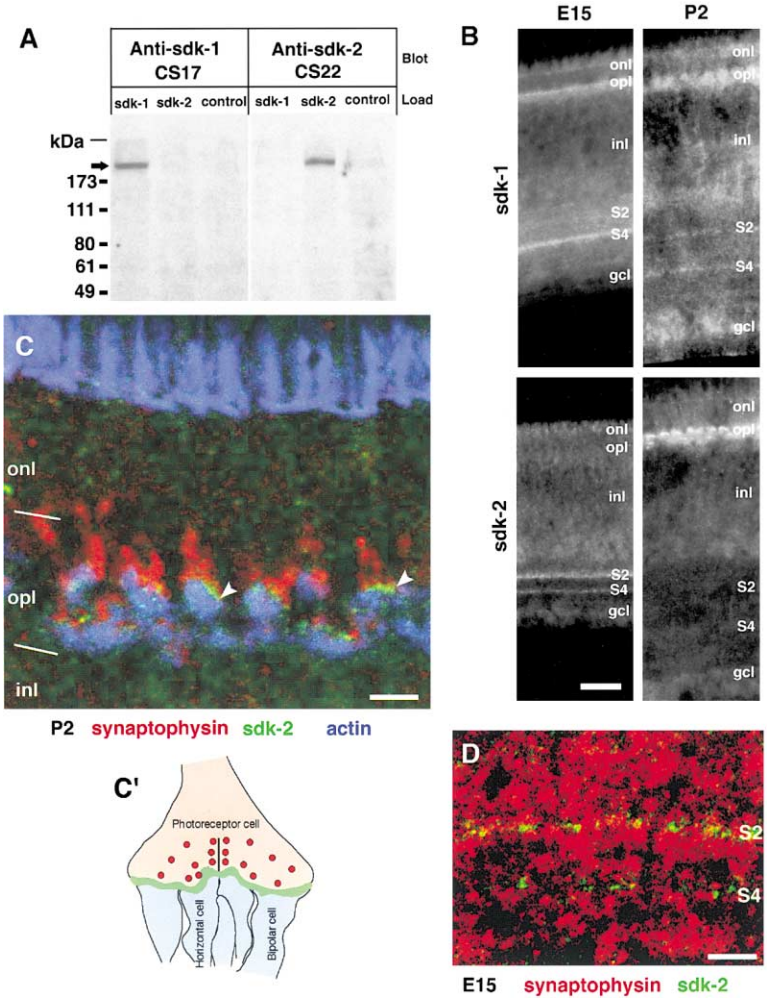

Figure 3. Sdks Are Concentrated at Synapses

(A) Specificity of monoclonal antobodies to Sdk-1 (CS17) and Sdk-2 (CS22) demonstrated by immunoblotting of cells that had been transfected with vectors encoding full-length Sdk expression vectors. "Control" lysate was made from untransfected cells. Both Sdk-1 and Sdk-2 migrated at ~240 kDa (arrow).

(B) Sections of chick retina at E15 or P2, stained with CS17 or CS22. Immunoreactivity is concentrated in the opl and in narrow bands within the ipl. Opl, outer plexiform layer; other abbreviations are as in Figure 2 legend. Bar equals 30 μm.

(C) Confocal microscopy of opl in retina triply stained with anti-Sdk-2 (green), anti-synaptophysin (red, to label nerve terminals), and phalloidin (blue, to stain the postsynaptic apparatus). Sdk-2 is concentrated in or near the synaptic cleft, sandwiched between pre- and postsynaptic structures. Sketch in (C′) shows ultrastructure of synapses in opl. Bar equals 10 μm.

(D) Confocal microscopy of ipl double-stained with anti-Sdk-2 and anti-synaptophysin. Sdk-rich puncta are restricted to narrow bands in sublaminae S2 and S4. Bar equals 10 μm.

bands were coincident. We also tested several markers expressed by subsets of amacrine cells. One, the calcium binding protein calbindin (Ellis et al., 1991), was present in the Sdk-1- and Sdk-2-positive bands; its relative intensity (S2 < S4) most resembled that of Sdk-1. Others marked only Sdk-negative sublaminae. For example, substance P (SP) is present at high levels in a narrow band in S3 and at low levels in a narrow band in S1, but not at all in S2, S4, or S5. (Some RGCs are also SP positive, but their SP is confined to somata and dentrites and does not contribute to the IPL; data not shown.) A third pattern was exhibited by acetylcholinesterase and choline acetyltransferase (Layer et al., 1997). Like Sdks, these markers were present in S2 and S4, but in bands that were offset from the Sdk-positive bands. By analogy to the physiologically well-characterized mammalian retina, S2 and S4 may be OFF and ON sublaminae, conveying information about the termination and onset of illumination, respectively (Layer et al., 1997; Masland, 2001).

Sdk-Expressing Neurons Project to Sdk-Positive Sublaminae

The restriction of Sdk protein to narrow bands in the IPL might reflect lamina-specific arborization of processes or lamina-specific localization of the protein within arbors that span multiple sublaminae. Unfortunately, distinguishing these alternatives was not simple: in situ hybridization marks cell somata but not processes, whereas Sdk protein is restricted to synapses. We therefore developed a technique for combining in situ hybridization with intracellular filling (see Experiment Procedures), so we could map dendritic arborizations of *sdk*-positive cells (Figure 5C). Sublaminar assignments were made by dividing the IPL into five equal subdivisions; thus, the Sdk-positive bands (36% ± 5% and 66% ± 2%, see above) were contained within S2 (20%–40%) and S4 (60%–80%). All ten *sdk-1*-positive cells mapped in this way had dendrites that arborized wholly or partly in S4. All 11 *sdk-2*-positive cells arborized in S2 and/or S4; six of them were bistratified, with arbors in both S2 and S4. As a control, we labeled cells with a mixture of *sdk-1* and *sdk-2* probes, then mapped dendritic arbors of cells that expressed neither *sdk* gene. These cells displayed a variety of dendritic patterns, with no marked preference for the Sdk-positive sublaminae.

Five double-labeled *sdk*-positive amacrines (two *sdk-1* and three *sdk-2*) were also identified in our material, all of which had processes in the Sdk-positive IPL sublaminae (Figure 5D). The inner nuclear layer is deep

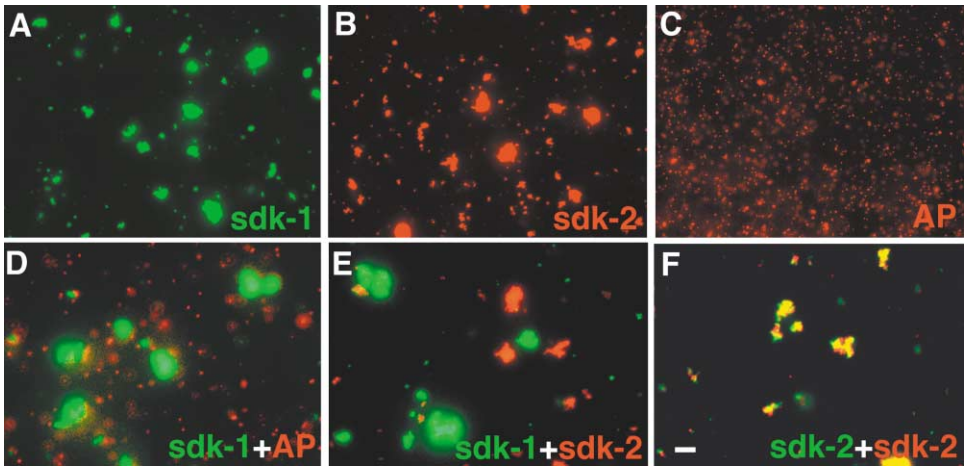

Figure 4. Sdk Proteins Mediate Homophilic Adhesion

Fluorescent polystyrene microspheres were coated with purified ectodomains of Sdk-1, Sdk-2, or alkaline phosphatase (AP), then incubated with gentle agitation for 1 hr. Beads coated with Sdk-1 (A) or Sdk-2 (B and F) aggregate. AP-coated beads do not aggregate (C), nor are they recruited into aggregates by Sdk-2 (D). When incubated together, Sdk-1 (green) and Sdk-2 (red) beads form separate aggregates (E), showing that homophilic adhesion predominates over heterophilic adhesion. Bar equals 20 μm for (A)–(C) and 10 μm for (D)–(F).

within the tissue, however, so cells in it were labeled less frequently than RGCs by the biolistic method. We therefore incubated retinae with anti-Sdk antibodies in organ culture to enhance staining or trap Sdk proteins in cellular processes. In this way, we occasionally labeled Sdk-positive cells, and in these cases, their processes terminated in S2 or S4 (Figure 5E and data not shown). Thus, Sdk-positive amacrine, bipolar, and RGCs selectively arborize in S2 and S4. Taken together, these results support, although they do not prove, the idea that Sdk-positive synapses connect pre- and postsynaptic cells that are both Sdk positive.

Ectopic Sdk Expression Diverts Processes to Sdk-Positive Sublaminae

If Sdk proteins interact homophilically in restricted sublaminae, they could participate in the generation or maintenance of lamina-specific connectivity. To test this possibility, we ectopically expressed Sdk-1 in Sdk-negative cells. An expression vector encoding *sdk-1* was electroporated in ovo at E2, before retinal neurons were born, then eyes were fixed and sectioned at E16, after IPL laminae had formed. For the analysis, we took advantage of the facts that SP-positive amacrine cells project to S1 and S3, which are Sdk negative (Figures 5A and 5B), and that endogenous Sdk-1 protein is detectable only at synapses (Figure 3). Thus, by double-labeling sections with anti-Sdk-1 and anti-SP, we could localize small clusters of transfected cells (Sdk-1-positive) and then examine processes that were normally Sdk negative (SP-positive).

We scored 56 clusters of Sdk-overexpressing cells in sections from >30 retinae. In seven of these regions, SP-positive fibers formed a double band: some fibers were in the normally SP-positive S3, but others were in Sdk-1-rich S4 (Figures 6A–6C). Thus, overexpression of Sdk-1 did not prevent expression of a S3 marker, but instead diverted processes bearing that marker to a novel destination. Presumably, in many of the phenotypically normal regions, the cluster of Sdk-1-overexpressing cells did not include any SP-positive cells, which comprise only a few percent of all amacrines.

Three controls were included in this set of experiments. First, to test whether intrinsic variability could account for the results, we examined the distribution of SP in thousands of untransfected regions in retinae that had been electroporated with *sdk-1*. In no case was a doubled band of SP-positive fibers observed. Second, to test whether transfection per se perturbed the SP-positive cells, we examined the distribution of SP in retinae transfected with a vector that encoded GFP. No displacements were seen in 42 transfected areas (Figures 6D–6F). Finally, to test whether Sdk has global effects on retinal development or lamination, we stained *sdk*-transfected retinae with antibodies to markers specific for RGCs (Brn 3), RGC and amacrine subsets (acetylcholine receptor β2), the optic fiber layer (neurofilaments), amacrine subsets (choline acetyltransferase and calbindin), and photoreceptors (visinin). In no case did we observe abnormalities in the region of Sdk-expressing cells (data not shown). Particularly compelling were results with calbindin. Calbindin-expressing amacrine cells normally arborize in Sdk-positive sublaminae (Figures 5A and 5B), so any displacement of their processes would indicate a nonspecific effect of Sdk overexpression. However, no such displacement was seen in 30 transfected areas (Figures 6G–6I).

In analyzing the experiments shown in Figure 6, we were struck by the fact that GFP-positive processes in the IPL usually spanned multiple sublaminae, whereas Sdk-overexpressing processes were generally restricted to a single sublamina (compare Figures 6A, 6D, and 6G). Since processes of most individual amacrines and RGCs are restricted to one or a few sublaminae, the diffuse pattern probably reflected the fact that each cluster contained a mixture of cell types. Likewise, the restricted pattern suggested that Sdk overexpression had diverted processes of multiple cell types to a single sublamina.

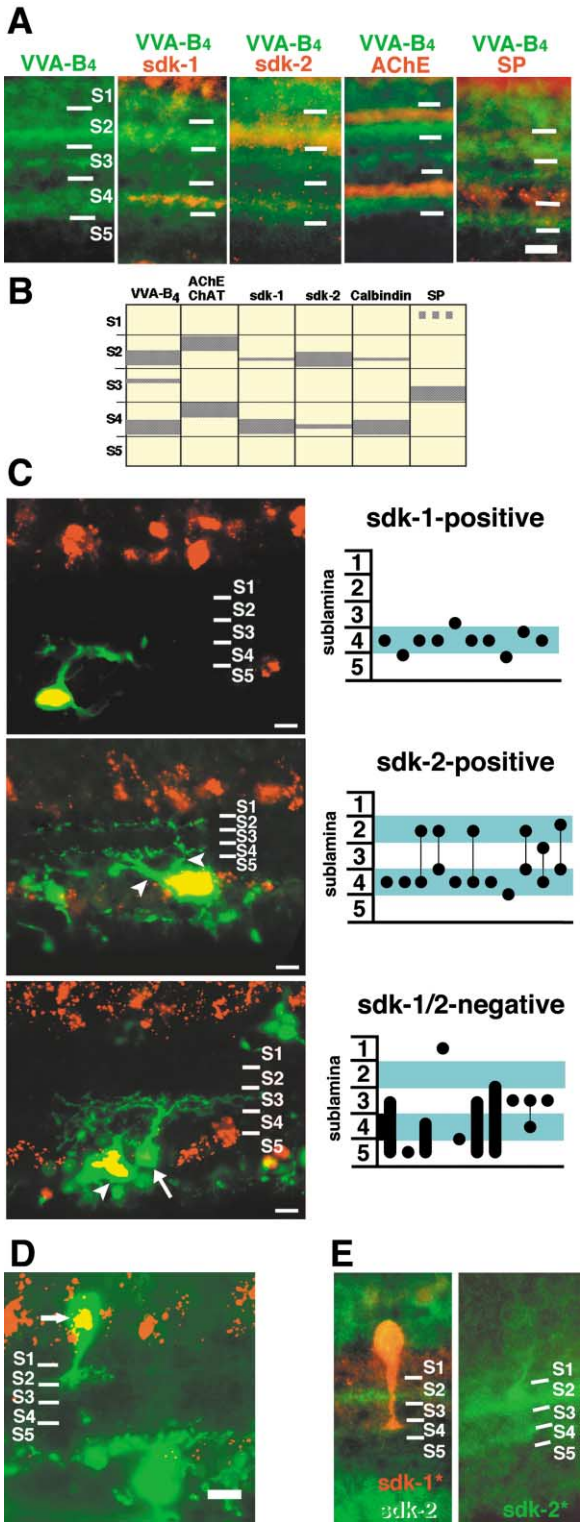

Figure 5. Characterization of Sdk-Positive Internal Plexiform Sublaminae

(A and B) Sublaminae in the IPL were characterized by double-staining with antibodies plus a lectin, VVA-B4. (A) shows examples and (B) is a summary. VVA-B4 stains thick bands in S2 and S4 and a thin band in S3. Sdk-1 and Sdk-2 stain the VVA-B4-positive bands in S2 and S4, with Sdk-2 predominating in S2 and Sdk-1 predominating in S4. Calbindin-positive bands overlap the Sdk/VVA-B4-positive bands in S2 and S4. Acetylcholinesterase (AChE) is also concentrated in S2 and S4, but stains bands distinct from those positive for Sdk and VVA-B4. Substance P (SP) is concentrated at the outer edge of S1 and at the base of S3. Bar equals 5 μm.

(C) Dendrites of *sdk*-positive RGCs arborize in S2 and S4. Cells were filled with fluorescein-conjugated dextran, then sections were processed for in situ hybridization with *sdk-1* and/or *sdk-2* probes. *Sdk-1*-postive, *sdk-2*-positive, or double-negative cells were identified and their dendrites mapped. Micrographs show examples and graphs summarize data from all cells. Arrowheads in the central panel mark two dendrites from a single cell, one running to S2 and the other to S4. Arrow and arrowhead in the bottom panel mark the cell that was scored and a neighboring *sdk*-positive cell, respectively. Thick dots or bars in graphs indicate arbors, and thin lines connect segments of bistratified arbors.

(D) A *sdk-2*-positive amacrine cell (arrow), labeled as in (C), with processes in S2. The same field contains a *sdk-2*-negative RGC with dendrites in S5.

(E) Amacrine cells incubated in organ culture with anti-Sdk (see Experimental Procedures). Left micrograph shows a Sdk-1-positive cell with processes in S4; right micrograph shows a Sdk-2-positive cell with processes in S2. In both cases, sections were restained with anti-Sdk-2 to mark S2 and S4. Bars in (C)–(E) equal 10 μm.

We therefore reasoned that assessing the distribution of Sdk-overexpressing processes in the IPL would provide a second test of the role of Sdks in IPL lamination. Importantly, this test would be more general because it did not depend on transfection of a rare cell type (SP-positive amacrines). Accordingly, we generated vectors that encoded both Sdk and GFP in a bicistronic message (*sdk-1*-ires-*gfp* or *sdk-2*-ires-*gfp*), as well as a vector that was identical except for lacking *sdk* (ires-*gfp*). Retinae were electroporated and sectioned as above; sections were stained with anti-GFP (because intrinsic GFP fluorescence was insufficiently bright after this long interval) and anti-Sdk-2 (to mark Sdk-positive bands in S2 and S4). A total of 360 clusters of GFP-labeled cells from 35 retinae were scored (Figures 7A and 7B).

When GFP was expressed alone, labeled processes usually spanned multiple laminae (66% of clusters; designated "D" for "diffuse"). In marked contrast, only a small fraction of clusters displayed a diffuse pattern of labeling in the IPL following transfection with *sdk-1*-ires-*gfp* or *sdk-2*-ires-*gfp* (16%). Instead, processes in most clusters were restricted to S2 or S4, the sublaminae to which endogenous Sdk-1 and Sdk-2 are restricted (62% and 68%, respectively). A subset of the Sdk-1-expressing clusters were double-stained for SP and GFP and, as above, expression of Sdk-1 led to a shift of SP-positive processes toward the ganglion cell layer (data not shown). These results support the idea that ectopic expression of either Sdk directs the processes of multiple types of amacrine, bipolar, and ganglion cells to Sdk-positive sublaminae. Although the difference was not statistically significant, there was a tendency for Sdk-1-overexpressing processes to terminate in S4, which is richest in endogenous Sdk-1, and for Sdk-2-overexpressing processes to terminate in S2, which is richest in endogenous Sdk-2 (compare Figures 3B and 7B).

Discussion

In a search for genes expressed by subsets of RGCs, we identified *sdk-1* and *sdk-2*. Their expression patterns

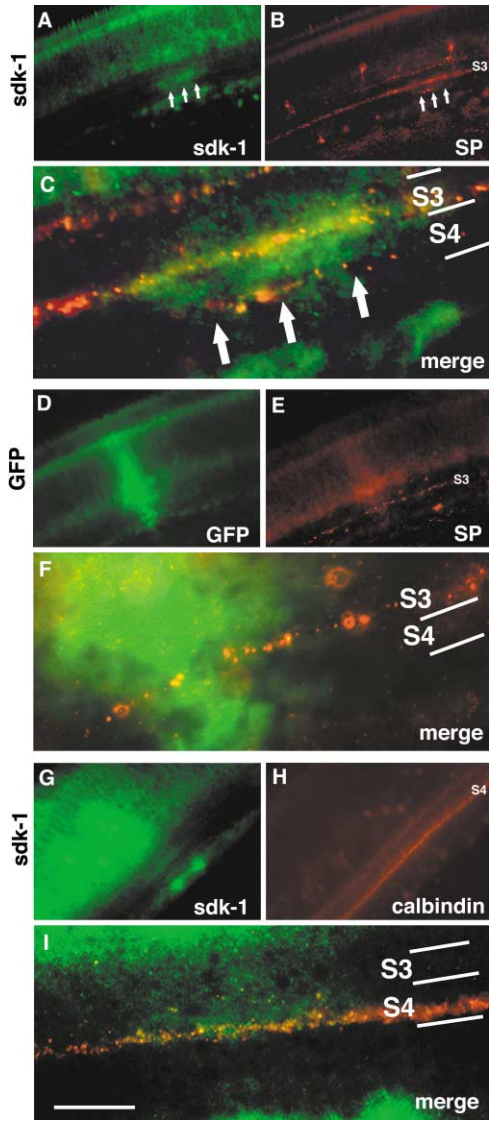

Figure 6. Sdk-1 Diverts Terminal Arbors from Sdk-Negative to Sdk-Positive Sublaminae without Changing Their Sublamina-Specific Molecular Identity

Embryos were electroporated in ovo at E2 with vectors encoding GFP or Sdk-1, then sections were stained at E16 with anti-Sdk-1, anti-substance P (SP), anti-calbindin, or anti-GFP as indicated. Terminals of SP-positive amacrine cells are normally confined to S1 and S3; some are diverted to S4 by ectopic expression of Sdk-1 (A–C, arrows). This diversion does not reflect a heightened lability of SP-positive arbors since GFP alone does not affect their position (D–F), nor does it reflect a nonspecific perturbation by Sdk, since calbindin-positive arbors (already in S2 and S4) are not diverted (G–I). (C), (F), and (I) show high-power merged images of the IPL from fields shown at lower power in (A) and (B), (D) and (E), and (G) and (H), respectively. Note that Sdk-overexpressing processes are clustered in a single sublamina (A and G), whereas GFP-expressing processes span multiple sublaminae (D). Bar in (I) equals 50 μm for (A), (B), (D), (E), (G), and (H) and 10 μm for (C), (F), and (I).

are noteworthy in several respects: the genes are expressed in nonoverlapping subsets of retinal neurons, both proteins are highly concentrated at synapses, and the Sdk-positive synapses in the IPL are restricted to clearly defined sublaminae. These features, along with their structure (reminiscent of known axon guidance molecules) and bioactivity in vitro (as mediators of homophilic adhesion) suggested that Sdks might be involved in the generation of lamina-specific connections. Tests in vivo supported this idea.

Sdks as Adhesion Molecules

The primary structure of Sdks provided the first clues to their function: they are type I transmembrane molecules with six Ig-like domains in their extracellular segments. This structure places them in the Ig superfamily, many of whose members mediate intercellular adhesion. Within this superfamily, Sdks belong to a large subfamily in which FN-III domains separate the Ig domains from the membrane. This family includes L1/NgCAM, DS-CAM, LAR, and Robo, all of which have been implicated in axon guidance (Walsh and Doherty, 1997; Kamiguchi and Lemmon, 2000; Kaprielian et al., 2000).

Assays with purified proteins confirmed that Sdks are adhesive. In our assays, both Sdk-1 and Sdk-2 interacted homophilically but not heterophilically. However, we have no absolute measure of the sensitivity of our adhesion assays, so we cannot rule out the possibility that Sdk-1 and Sdk-2 adhere to each other weakly. Moreover, we have not tested the ability of Sdks to bind other molecules. Several Ig superfamily cell adhesion molecules adhere to distant relatives and unrelated molecules (Kamiguchi and Lemmon, 2000). In addition, some Ig/FN-III proteins have carbohydrate as well as protein ligands. A consensus sequence in the FN-III domain is believed to mediate this lectin-like activity (LxPxxxYxFRVxAxNxxG; Kleene et al., 2001) and both Sdks bear this sequence.

Although vertebrate *sdks* are members of a large family, the only known genes that are closely related in sequence or domain structure (six C2-type Ig domains followed by 13 FN-III repeats) are fly and nematode *sdks*. The fly gene was identified in a screen for mutants with defects in eye development, which is noteworthy in view of the roles described here. Further insight into the functions of vertebrate Sdks may eventually come from the fly ortholog, but neither its primary site of action nor its pattern of expression has yet been determined (Nguyen et al., 1997). The *C. elegans* ortholog is predicted from genomic sequence, but its transcription has not been verified.

Sdks at Synapses

The most striking feature of Sdk protein localization is its concentration at synapses. Our antibodies have not proven suitable for electron microscopic immunohistochemistry, but confocal microscopy of the large photoreceptor synapses in the outer plexiform layer strongly supports the notion that Sdk ectodomains are located in the synaptic cleft. Sdks therefore join a small group of proteins likely to mediate interactions between pre- and postsynaptic elements at central synapses. Some, like cadherins (Yamagata et al., 1995; Fannon and Colman, 1996; Uchida et al., 1996) potentially connect cells that express the same protein. Others, like neuroligin and neurexin (Irie et al., 1997; Scheiffele et al., 2000) or ephrin B and ephB kinase (Torres et al., 1998; Dalva et al., 2000) form inherently asymmetric junctions. In view

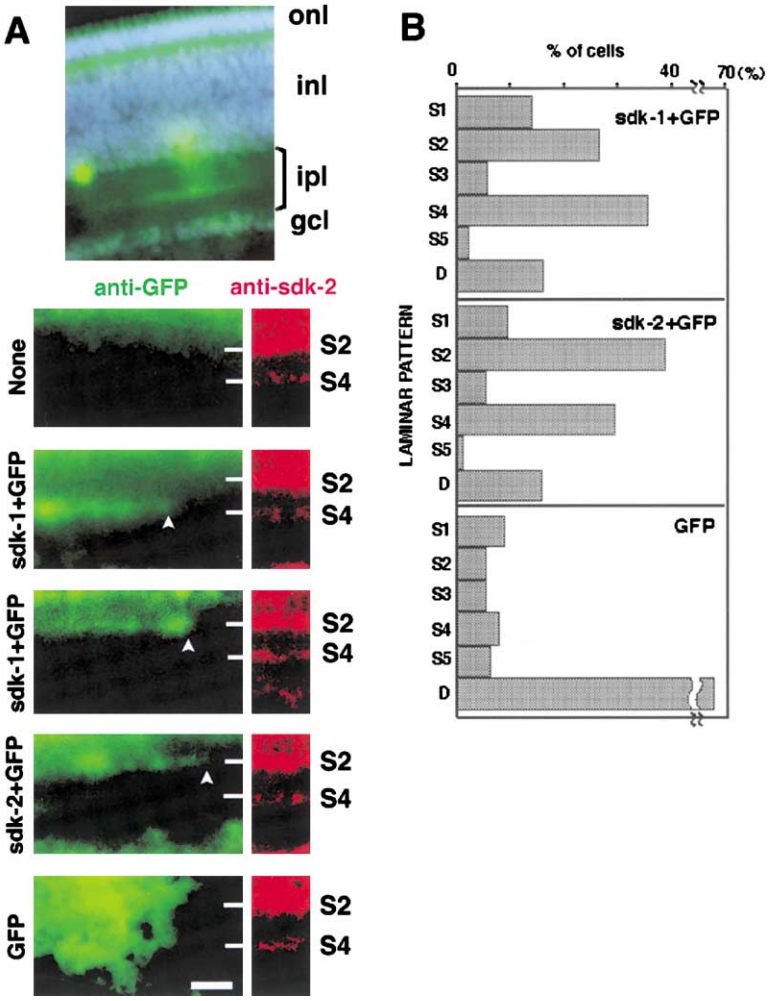

Figure 7. Sdk-Overexpressing Neurites Stratify in Sdk-Positive Sublaminae

(A) Embryos were electroporated in ovo at E2 with vectors encoding Sdk-1 and GFP (*sdk-1*-ires-*gfp*), Sdk-2 and GFP (*sdk-2*-ires-*gfp*), or GFP alone. At E16, sections were stained with anti-GFP (green) to visualize processes of transfected cells (arrowheads), anti-Sdk-2 (red) to visualize S2 and S4, and DAPI. In retinae overexpressing only GFP, labeled processes were distributed diffusely because multiple cells with diverse morphologies were GFP positive within each cluster. In contrast, GFP-labeled processes were largely restricted to S2 or S4 when the vector encoded Sdk-1 or Sdk-2 in addition to GFP. Sections of untransfected retina shows that the antibody to GFP stained nuclear layers but not IPL nonspecifically. The top micrograph shows a low-power view from a retina transfected with *sdk-1*-ires-*gfp*; other micrographs are higher-power views of the IPL. Abbreviations are as in Figure 2. Bar equals 10 μm.

(B) Laminar restriction of GFP-positive processes in transfected retinae, as scored from sections similar to those in (A). D (diffuse) indicates that processes were not restricted to specific sublaminae. n = 87–111 per panel.

of the homophilic nature of Sdks and the likelihood that Sdk-positive synapses connect pairs of Sdk-expressing cells, we speculate that Sdks are in the former class.

The mechanisms that restrict Sdks to synaptic membranes are unknown, but the primary sequence suggests one possibility. All known Sdks (two human, two mouse, two chick, one fly, and one nematode) terminate in the sequence GFSSFV. The final three of these residues correspond to the consensus sequence for binding to PDZ domains (-S/TxV-COOH). PDZ proteins serve as scaffolds to bind, accumulate, and coordinate components of specialized intercellular contacts, with synapses prominent among them. Many synapse-associated cytoplasmic proteins (e.g., PSD-95, Homer, and GRIP) contain PDZ domains, and many synaptic membrane proteins (e.g., glutamate receptors, neuroligin, and neurexin) interact with these domains via carboxy-terminal S/TxV motifs (reviewed in Sheng and Sala, 2001). By analogy, the synaptic localization of Sdks is likely to be mediated and/or stabilized by interactions with synaptic PDZ proteins. Moreover, residues immediately adjacent to the S/TxV motif are determinants of the particular PDZ domains to which a given protein binds (Sheng and Sala, 2001). The conservation of the carboxy-terminal hexapeptide in all Sdks therefore suggests that they bind preferentially to a specific subset of synaptic PDZ domains. Together, the synaptic localization and homophilic adhesive properties of Sdks support the idea that they play roles in the formation or maintenance of a subset of retinal synapses (Figure 8A).

Sdks and Laminar Specificity

As noted in the Introduction, the IPL provides a striking example of lamina-specific (and perhaps lamina-specified) connectivity. The notion that Sdks are involved in laminar specificity was initially suggested by the restriction of Sdk-positive synapses to two narrow bands within the IPL. Findings consistent with this idea are that Sdks accumulate at these sites as sublaminae are forming and that Sdks are homophilic adhesion molecules of the synaptic cleft. To assess the role of Sdks in vivo, we tested the effects of expressing them in retinal cells that were normally Sdk negative. In two separate assays (one examining all Sdk-overexpressing processes and one examining a specific marker of normally Sdk-negative amacrine cells), we found that Sdk expression diverted processes to Sdk-positive sublaminae. Importantly, this diversion represents a rerouting of processes, not an overall change in neuronal identity, as assessed by continued neuropeptide (SP) expression

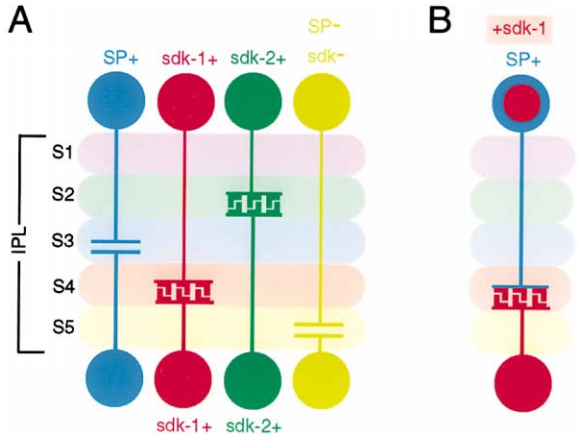

Figure 8. Proposed Roles of Sdks in Sublamina-Specific Connectivity

(A) Sdks could stabilize synapses in the IPL. Subsets of cells in the inner nuclear layer send neurites to one or a few sublaminae in the IPL, where they synapse on subsets of RGCs whose dendrites are similarly lamina restricted. Sdk-1- and Sdk-2-positive populations project predominantly to S4 and S2, respectively, where their synaptic membranes bear Sdk protein. (Some Sdk-1-positive cells also project to S2 and some Sdk-2-positive cells project to S4; not shown.) Sdk-negative subsets project to other sublaminae, including the SP-positive amacrines that project to S3. In the narrow Sdk-positive bands within S2 and S4, homophilic interactions of Sdk proteins in the synaptic cleft could contribute to intercellular adhesion or signaling between pre- and postsynaptic elements.

(B) Sdks could promote lamina-specific specific connectivity. Forced expression of Sdk-1 or -2 in retinal cells diverts their processes to the Sdk-positive S2 or S4. For example, expression of Sdk-1 in SP-positive amacrines that normally project to S3 diverts their neurites to S4. Thus, Sdks may contribute to synaptic specificity as well as to synapse formation per se.

(Figure 8B). These results provide strong evidence that Sdks can modulate, and may perhaps mediate, laminar specificity.

Three complications to this simple conclusion need to be noted. First, Sdk-1 and Sdk-2 are present in the same two sublaminae, and therefore have the opportunity to interact with each other. However, Sdk-1 and Sdk-2 are expressed in distinct cells and do not interact detectably in vitro. We therefore favor the view that Sdks not only promote lamina-specific connections but also segregate Sdk-1- and Sdk-2-positive connections within the same sublamina. Second, only 2 of ≥10 IPL bands bear detectable Sdk protein. Given the absence of additional *sdk* genes in mouse and human genomes, Sdks are surely not the sole determinants of laminar targeting in the IPL. No other determinants have been identified to date, but promising candidates include cadherins (Wohrn et al., 1998). Third, we have assessed the effect of adding a Sdk to Sdk-negative cells (gain-of-function tests) but not the effect of removing it from Sdk-positive cells (loss-of-function tests). Therefore, we can conclude that Sdks are sufficient for laminar targeting of retinal processes, but not that they are necessary. If Sdks are components of an overdetermined system for ensuring specific connectivity, their loss might not disrupt lamination. For technical reasons, we plan to perform loss-of-function analysis in mice.

What developmental steps do Sdks affect? The simplest hypothesis is that Sdks promote synapse formation between Sdk-positive pre- and postsynaptic partners. Because Sdks are present in the IPL as soon as sublaminae appear, however, they could play additional roles. For example, dendrites of RGCs that belong to the same morphological or physiological class fasciculate with each other in a pattern suggestive of homophilic adhesive interactions (Lohmann and Wong, 2001). Sdks could contribute to these interactions, or similar interactions amongst amacrine processes, compressing them into a narrow plate and thereby helping to *form* sublaminae. Another possibility is that Sdks refine initially diffuse arbors. Several recent studies have suggested that amacrine cells play the lead roles in sublamina formation, with RGC dendrites gradually remodeling to match the amacrine scaffold (Gunhan-Agar et al., 2000; Williams et al., 2001). If this view is correct, presynaptic Sdks might form a scaffold that dendritic Sdks recognize. Moreover, synaptically driven activity in RGCs promotes their dendritic remodeling (Bisti et al., 1998), raising the possibility that recognition of Sdk or responses to it are regulated by synaptic activity.

Finally, in addition to helping illuminate developmental processes, Sdks may be useful in analyzing information processing in the visual system. Circuitry in the IPL is "an ordered stack of synaptic planes, more like a club sandwich than a tangle of spaghetti" (Masland, 2001). Each of its sublaminae comprises a representation of the visual world that is conveyed through its bipolar and amacrine cells inputs, modified by vertical interactions amongst sublaminae, and passed to the brain through distinct subsets of RGCs (Boycott and Wassle, 1999; Roska and Werblin, 2001). Thus, the IPL performs parallel processing in the most literal sense. Molecular labels can supplement physiological analysis of this processing by providing means to trace projections of, record from, or selectively ablate specific subpopulations. The power of these approaches is shown by several recent studies of amacrine and bipolar subsets, for which some molecular tags are available (for example, Nirenberg and Meister, 1997; Yoshida et al., 2001). Sdks may be the first markers of RGCs that project to specific IPL sublaminae, and are surely the first to mark pre- and postsynaptic cells that target the same sublaminae. They may, therefore, provide new reagents for targeted manipulation of retinal circuitry.

Experimental Procedures

Identification and Analysis of *sdk* cDNAs

Single retinal ganglion cells were obtained from E14 chick retina by dissociation with papain, and immunopurification with a mouse monoclonal antibody to thy-1 (BSJ-1; French and Jeffrey, 1986) coupled to goat anti-mouse IgG microbeads (MACS, 484-02, Miltenyi Biotec). RNA from individual cells was reverse-transcribed and amplified by the method of Dulac and Axel (1995). PCR products were cloned into λ ZAPII phages, and selected libraries were differentially screened with probes from single-cell RT-PCR products. A detailed protocol will be published elsewhere (J.A.W., M.Y., C. Dulac, K. Roth, and J.R.S., unpublished data).

To obtain the entire *sdk* open reading frames, we generated a cDNA library from E14 chicken retina in the λUni-ZAPII vector (Stratagene). Additional mouse and human *sdk* sequence was obtained from the Celera Genomics database (http://www.celera.com). Do-

main structure was predicted using Pfam 6.6 (http://pfam.wustl.edu/). The ClustalW algorithm (Lasergene software package, DNA Star) was used for alignments.

In Situ Hybridization and Intracellular Filling

Riboprobes were synthesized using either digoxigenin- or fluorescein-labeled UTP, then hydrolyzed to ~500 nt. Sections were prepared and hybridized at 65°C by the method of Schaeren-Wiemers and Gerfin-Moser (1993). For double-labeling, probes were hybridized together and detected sequentially using anti-digoxigenin or anti-fluorescein antibodies conjugated to peroxidase, followed by amplification with FITC-tyramide and Cy3-tyramide (TSA-Plus system; Perkin-Elmer Life Sciences). Following the first signal detection, the antibody-conjugated peroxidase was inactivated with 0.3% H_2O_2 for 40 min. Control experiments demonstrated the efficacy of this inactivation and confirmed that all labeling from the second tyramide reaction was due to the second peroxidase-conjugated antibody.

To visualize the processes of *sdk*-positive cells, in situ hybridization was combined with biolistic intracellular filling. Tungsten particles (1.3 μm) were coated with fluorescein-conjugated dextran (10,000 MW; Molecular Probes, dissolved in water at 125 mg/ml), coated onto plastic cartridges, and loaded into a BioRad Helios Gene Gun. E16 retinae were quartered and flat-mounted, vitreal-side up, onto nitrocellulose filters (Millipore) in oxygenated chick Ringer's solution. Retinae were shot through a 3 μm membrane filter (Becton-Dickinson) using 80 psi helium gas, incubated in oxygenated chick Ringer's for 1 hr in the dark, fixed for 1 hr with 4% paraformaldehyde, cryoprotected in 20% sucrose, and frozen for cryostat sectioning at 20 μm. Sections were processed for in situ hybridization as above, using digoxigenin-labeled riboprobes to *sdk-1*, *sdk-2*, or both. Finally, the dextran signal was enhanced using anti-fluorescein-peroxidase and FITC-tyramide as above.

Immunohistochemistry

cDNA fragments encoding the fifth and sixth immunoglobulin domains and first 2 FN-III repeats of chicken Sdk-1 (aa 471–762) or Sdk-2 (aa 464–779) were cloned into a TriEx-1 vector (Novagen), which contains a polyhistidine epitope tag. Recombinant proteins were expressed in *E. coli*, purified with HisBond (Novagen), and used to immunize Balb/c mice for generation of monoclonal antibodies.

Retinae were fixed with 4% paraformaldehyde/PBS for 2 hr at 4°C, sunk in 15% and 30% sucrose/PBS, frozen in OCT, and sectioned at 20 μm in a cryostat. Sections were treated with 0.1% (w/v) Triton X-100 in PBS for 10 min at room temperature, blocked with 5% skim milk in PBS for 30 min, and incubated successively with primary and secondary antibodies. For CS17, sections were pretreated with 8 M urea, 50 mM TrisHCl (pH 7.4), for 10 min at room temperature. For fluorescein-conjugated VVA-B4 (Sigma), 1% BSA in PBS was used instead of skim milk as blocking solution. Nuclei were counterstained with DAPI (4′-6-diamidino-2-phenylindole). Actin was labeled with Alexa 660-conjugated phalloidin (Molecular Probes). For the experiment shown in Figure 5F, retinae were cultured in the presence of anti-Sdk for 12 hr at 37°C before being fixed and sectioned.

Aggregation Assay

cDNAs encoding the complete ectodomains of Sdk-1 and Sdk-2 were transfected into human embryonic kidney 293T cells and his-tagged proteins were purified from cell lysates using Ni-NTA resins (Novagen). Fluoresbrite YG 1.0 μm or PolyFluor 570 microspheres (Polysciences) were coated with purified proteins by overnight incubation, collected by centrifugation, and dispersed by sonication immediately before each assay. For the assay, 10 μl aliquots of microspheres were rotated at 60 rpm for 1 hr at room temperature in 60-well Terasaki plates (Nunclon).

Electroporation In Ovo

The IRES2-EGFP sequence was excised from pIRES2-EGFP vector (Clontech) and appended to the 3′ end of *sdk* cDNAs in the TriEx-1 plasmid. Plasmids (2 μg/μl) were mixed with an *E. coli* β-galactosidase expression vector and the mixture was injected into the anterior neural tubes of Hamburger-Hamilton stage 9–10 (E2) chick embryos. A 5 mm length, 0.5 mm diameter stainless steel electrode was placed parallel to the neural tube, the tip of a tungsten needle cathode was inserted into the lumen of the neural tube, and 3 unipolar square pulses (25 mS, 7V) were delivered using a ECM830 electroporator (BTX), with the tungsten electrode as cathode (Momose et al., 1999). With this method, >50% of electroporated embryos survived to E16, at which point retinae were fixed for 1 hr at 4°C and stained with X-gal for 2 hr. Regions containing transfected (blue) cells were found in ~10% of the retinae; these were dissected, refixed with 4% paraformaldehyde/PBS for 30 min, then cryosectioned and stained as above.

Acknowledgments

We thank Catherine Dulac for advice on generation of single-cell libraries; K. Roth for advice on in situ hybridization; R. Wong, C. Lohmann, and R. Stacy for advice on retinal anatomy and biolistic methods; R. Lewis for DNA sequencing; and R. Rotundo for AChE antibody. This work was supported by an NRSA fellowship to J.A.W. and grants from NIH to J.R.S.

Received: April 5, 2002
Revised: August 1, 2002

References

Benson, D.L., Colman, D.R., and Huntley, G.W. (2001). Molecules, maps and synapse specificity. Nat. Rev. Neurosci. *2*, 899–909.

Bisti, S., Gargini, C., and Chalupa, L.M. (1998). Blockade of glutamate-mediated activity in the developing retina perturbs the functional segregation of ON and OFF pathways. J. Neurosci. *18*, 5019–5025.

Boycott, B., and Wassle, H. (1999). Parallel processing in the mammalian retina: the Proctor Lecture. Invest. Ophthalmol. Vis. Sci. *40*, 1313–1327.

Cajal, S.R. (1893). La retine des vertebres. Cellule *9*, 119–257.

Dalva, M.B., Takasu, M.A., Lin, M.Z., Shamah, S.M., Hu, L., Gale, N.W., and Greenberg, M.E. (2000). EphB receptors interact with NMDA receptors and regulate excitatory synapse formation. Cell *103*, 945–956.

Dulac, C., and Axel, R. (1995). A novel family of genes encoding putative pheromone receptors in mammals. Cell *83*, 195–206.

Ellis, J.H., Richards, D.E., and Rogers, J.H. (1991). Calretinin and calbindin in the retina of the developing chick. Cell Tissue Res. *264*, 197–208.

Fannon, A.M., and Colman, D.R. (1996). A model for central synaptic junctional complex formation based on the differential adhesive specificities of the cadherins. Neuron *17*, 423–434.

French, P.W., and Jeffrey, P.L. (1986). Partial characterization of chicken Thy-1 glycoprotein by monoclonal antibodies. J. Neurosci. Res. *16*, 479–489.

Gunhan-Agar, E., Kahn, D., and Chalupa, L.M. (2000). Segregation of on and off bipolar cell axonal arbors in the absence of retinal ganglion cells. J. Neurosci. *20*, 306–314.

Holt, C.E., and Harris, W.A. (1998). Target selection: invasion, mapping and cell choice. Curr. Opin. Neurobiol. *8*, 98–105.

Inoue, A., and Sanes, J.R. (1997). Lamina-specific connectivity in the brain: regulation by N-cadherin, neurotrophins, and glycoconjugates. Science *276*, 1428–1431.

Irie, M., Hata, Y., Takeuchi, M., Ichtchenko, K., Toyoda, A., Hirao, K., Takai, Y., Rosahl, T.W., and Sudhof, T.C. (1997). Binding of neuroligins to PSD-95. Science *277*, 1511–1515.

Kamiguchi, H., and Lemmon, V. (2000). IgCAMs: bidirectional signals underlying neurite growth. Curr. Opin. Cell Biol. *12*, 598–605.

Kaprielian, Z., Imondi, R., and Runko, E. (2000). Axon guidance at the midline of the developing CNS. Anat. Rec. *261*, 176–197.

Karten, H.J., Reiner, A., and Brecha, N. (1982). Laminar organization and origins of neuropeptides in the avian retina and optic tectum. In Cytochemical Methods in Neuroanatomy, V. Chan-Palay and S.L. Palay, eds. (New York: A. R. Liss), pp. 189–204.

Kleene, R., Yang, H., Kutsche, M., and Schachner, M. (2001). The

neural recognition molecule L1 is a sialic acid-binding lectin for CD24, which induces promotion and inhibition of neurite outgrowth. J. Biol. Chem. *276*, 21656–21663.

Layer, P.G., Berger, J., and Kinkl, N. (1997). Cholinesterases precede "ON-OFF" channel dichotomy in the embryonic chick retina before onset of synaptogenesis. Cell Tissue Res. *288*, 407–416.

Lohmann, C., and Wong, R.O. (2001). Cell-type specific dendritic contacts between retinal ganglion cells during development. J. Neurobiol. *48*, 150–162.

Masland, R.H. (2001). The fundamental plan of the retina. Nat. Neurosci. *4*, 877–886.

Millar, T.J., Ishimoto, I., Chubb, I.W., Epstein, M.L., Johnson, C.D., and Morgan, I.G. (1987). Cholinergic amacrine cells of the chicken retina: a light and electron microscope immunocytochemical study. Neuroscience *21*, 725–743.

Momose, T., Tonegawa, A., Takeuchi, J., Ogawa, H., Umesono, K., and Yasuda, K. (1999). Efficient targeting of gene expression in chick embryos by microelectroporation. Dev. Growth Differ. *41*, 335–344.

Nguyen, D.N., Liu, Y., Litsky, M.L., and Reinke, R. (1997). The sidekick gene, a member of the immunoglobulin superfamily, is required for pattern formation in the *Drosophila* eye. Development *124*, 3303–3312.

Nirenberg, S., and Meister, M. (1997). The light response of retinal ganglion cells is truncated by a displaced amacrine circuit. Neuron *18*, 637–650.

Roska, B., and Werblin, F. (2001). Vertical interactions across ten parallel, stacked representations in the mammalian retina. Nature *410*, 583–587.

Sanes, J.R., and Yamagata, M. (1999). Formation of lamina-specific synaptic connections. Curr. Opin. Neurobiol. *9*, 79–87.

Schaeren-Wiemers, N., and Gerfin-Moser, A. (1993). A single protocol to detect transcripts of various types and expression levels in neural tissue and cultured cells: in situ hybridization using digoxigenin-labelled cRNA probes. Histochemistry *100*, 431–440.

Scheiffele, P., Fan, J., Choih, J., Fetter, R., and Serafini, T. (2000). Neuroligin expressed in nonneuronal cells triggers presynaptic development in contacting axons. Cell *101*, 657–669.

Scott, L.J., Bacou, F., and Sanes, J.R. (1988). A synapse-specific carbohydrate at the neuromuscular junction: association with both acetylcholinesterase and a glycolipid. J. Neurosci. *8*, 932–944.

Sheng, M., and Sala, C. (2001). PDZ domains and the organization of supramolecular complexes. Annu. Rev. Neurosci. *24*, 1–29.

Sheppard, A.M., Konopka, M., Robinson, S.R., Morgan, I.G., and Jeffrey, P.L. (1991). Thy-1 antigen is specific to ganglion cells in chicks. Neurosci. Lett. *123*, 87–90.

Torres, R., Firestein, B.L., Dong, H., Staudinger, J., Olson, E.N., Huganir, R.L., Bredt, D.S., Gale, N.W., and Yancopoulos, G.D. (1998). PDZ proteins bind, cluster, and synaptically colocalize with Eph receptors and their ephrin ligands. Neuron *21*, 1453–1463.

Uchida, N., Honjo, Y., Johnson, K.R., Wheelock, M.J., and Takeichi, M. (1996). The catenin/cadherin adhesion system is localized in synaptic junctions bordering transmitter release zones. J. Cell Biol. *135*, 767–779.

Walsh, F.S., and Doherty, P. (1997). Neural cell adhesion molecules of the immunoglobulin superfamily: role in axon growth and guidance. Annu. Rev. Cell Dev. Biol. *13*, 425–456.

Williams, R.R., Cusato, K., Raven, M.A., and Reese, B.E. (2001). Organization of the inner retina following early elimination of the retinal ganglion cell population: effects on cell numbers and stratification patterns. Vis. Neurosci. *18*, 233–244.

Wohrn, J.C., Puelles, L., Nakagawa, S., Takeichi, M., and Redies, C. (1998). Cadherin expression in the retina and retinofugal pathways of the chicken embryo. J. Comp. Neurol. *396*, 20–38.

Yamagata, M., and Sanes, J.R. (1995a). Lamina-specific cues guide outgrowth and arborization of retinal axons in the optic tectum. Development *121*, 189–200.

Yamagata, M., and Sanes, J.R. (1995b). Target-independent diversification and target-specific projection of chemically defined retinal ganglion cell subsets. Development *121*, 3763–3776.

Yamagata, M., Herman, J.P., and Sanes, J.R. (1995). Lamina-specific expression of adhesion molecules in developing chick optic tectum. J. Neurosci. *15*, 4556–4571.

Yoshida, K., Watanabe, D., Ishikane, H., Tachibana, M., Pastan, I., and Nakanishi, S. (2001). A key role of starburst amacrine cells in originating retinal directional selectivity and optokinetic eye movement. Neuron *30*, 771–780.

Accession Numbers

The GenBank accession number for chicken *sdk-1* and *sdk-2* are AF537107 and AF537108.